

## Original Research Article

# MiR-486 protects against acute myocardial infarction via regulation of PTEN

Qinfeng Han<sup>1</sup>, Zhong Xu<sup>1</sup>, Xiaolei Zhang<sup>1</sup>, Kun Yang<sup>1</sup>, Zhifei Sun<sup>1</sup>, Weidong Sun<sup>1</sup>, Wanbo Liu<sup>2\*</sup>

<sup>1</sup>The Third Department of Cardiovascular Medicine, Taian City Central Hospital, Taian, <sup>2</sup>Department of Internal Medicine, Zhantansi Outpatient, Central Medical Branch of PLA General Hospital, Beijing, China

\*For correspondence: **Email:** [liuwanbo200@163.com](mailto:liuwanbo200@163.com); **Tel:** +86-018010216753

Sent for review: 8 April 2021

Revised accepted: 23 August 2021

### Abstract

**Purpose:** To investigate the effect of miR-486 on rats with acute myocardial infarction (AMI), and its mechanism of action.

**Methods:** A rat model of AMI was established. They were randomly divided into 4 groups, namely, sham, model, agomiR-486 and antagomiR-486 groups, respectively. Rats in these different groups were treated with agomiR-21 (5  $\mu$ L, 40 nmol/mL), antagomiR-21 (5  $\mu$ L, 40 nmol/mL) or agomiR-NC (5  $\mu$ L, 40 nmol/mL), respectively. Then, key miRNAs were sorted out using gene-chip assay and verified by quantitative reverse transcription polymerase chain reaction (qRT-PCR) assay. Luciferase reporter gene assay was conducted to determine the interaction between miR-486 and gene of PTEN. After intraperitoneal injection of agomiR-486 and antagomiR-486, hemodynamics was measured to determine the effect of miR-486 on myocardial function of the rats. The effect of miR-486 expression level on the expression of myocardial enzymes in serum, the morphology of myocardial tissues, and the apoptosis of myocardial tissues in rats, were investigated. Additionally, the effect of miR-486 expression level on PTEN/AKT signaling pathway in the rats was determined by Western blotting.

**Results:** The results of gene-chip and qRT-PCR assays revealed that there were 8 differentially expressed genes in rat myocardial tissues in the model group when compared with the sham group. MiR-486 improved the cardiac function of rats and the morphology of myocardial tissues, but reduced AMI-induced apoptosis of myocardial cells and the expression of myocardial enzymes (markers of myocardial injury) in a dose-dependent manner ( $p < 0.05$ ). The results of luciferase reporter gene assay showed that PTEN was a direct target of miR-486. In rat models of AMI, a raised expression of miR-486 remarkably suppressed the protein expression level of PTEN and up-regulated that of p-AKT/AKT ( $p < 0.05$ ).

**Conclusion:** MiR-486 protects against AMI in rats probably by targeting PTEN and activating the AKT signaling pathway. The results of the current study may provide new insights for the treatment of AMI.

**Keywords:** miR-486, PTEN, Acute myocardial infarction, p-AKT/AKT, Gene chip, PTEN/AKT signaling pathway

This is an Open Access article that uses a funding model which does not charge readers or their institutions for access and distributed under the terms of the Creative Commons Attribution License (<http://creativecommons.org/licenses/by/4.0>) and the Budapest Open Access Initiative (<http://www.budapestopenaccessinitiative.org/read>), which permit unrestricted use, distribution, and reproduction in any medium, provided the original work is properly credited.

Tropical Journal of Pharmaceutical Research is indexed by Science Citation Index (SciSearch), Scopus, International Pharmaceutical Abstract, Chemical Abstracts, Embase, Index Copernicus, EBSCO, African Index Medicus, JournalSeek, Journal Citation Reports/Science Edition, Directory of Open Access Journals (DOAJ), African Journal Online, Bioline International, Open-J-Gate and Pharmacy Abstracts

## INTRODUCTION

Coronary heart disease, also known as ischemic heart disease, is one of the diseases with the highest morbidity and mortality rates worldwide, which manifests as the narrowing and remodeling of the coronary arteries, leading to ischemia and hypoxia in the myocardium and thus inducing acute myocardial infarction (AMI) [1]. Besides, its clinical manifestations include unstable angina pectoris, non-ST-segment elevation AMI (NSTEMI), ST-segment elevation AMI (STEMI) and sudden cardiac death [2].

Current epidemiological studies have demonstrated that AMI has an obvious association with various related factors like age, gender, lifestyle, hypertension, diabetes, atherosclerosis, dyslipidemia and genetic factors [3], which have complex pathogenesis, are high risk and could lead to a high disability as well as mortality rate among patients if treatment is belated. Moreover, AMI caused by insufficient blood supply easily leads to myocardial tissue necrosis, inflammatory response, pathological myocardial remodeling and ultimately, heart failure. However, the exact molecular mechanisms of the pathophysiological process of AMI is not yet fully elucidated. As a result, exploring and studying the pathological mechanism of AMI and finding out key molecules therein are crucial for developing effective therapeutic and preventive methods.

Micro ribonucleic acids (miRNAs) are a class of non-coding RNAs with a small molecular weight, the mechanism of action of which is to bind to the 3'-untranslated region (3'-UTR) of messenger RNAs (mRNAs) to repress the expression of mRNAs or induce their degradation, ultimately modulating a series of important biological processes, including energy metabolism and cell growth, survival and differentiation [4]. At present, numerous studies have pointed out that miRNAs play extremely important roles in the pathological process of cardiovascular diseases. For instance, a clinical study showed that changes in miR-1 expression level in blood are of potential diagnostic value in the development of AMI, which are independent risk factors for the prognosis of AMI and can be used to predict the prognosis of AMI [5].

An *in vivo* study on myocardial infarction in rats indicated that increased expression of miR-133a can reduce the mRNA and protein levels of TGF- $\beta$ 1 and CTGF after myocardial infarction, decreasing myocardial collagen deposition, inhibiting myocardial fibrosis and improving heart function [6]. In addition, a study suggested that

miR-496 is able to resist myocardial apoptosis by targeting Hook3 and activating the phosphatidylinositol 3-kinase (PI3K)/AKT/mTOR signaling pathway [7].

Therefore, discovering important miRNAs which regulate the pathological process of AMI and exploring their mechanisms of action, are critical to the further understanding of the pathological mechanism of AMI, which will provide opportunities for the development of new drugs and new molecular markers for diagnosis and prognosis.

## EXPERIMENTAL

### Modeling of AMI in rats

A total of 40 SD male rats weighing 180 - 200 g were housed in an SPF-grade animal room at 25 °C and a humidity of 45 % under a light-dark cycle of 12 h/ 12 h with free access to feed and water. They were randomly divided into 4 groups, namely, sham, model, agomiR-486 and antagomiR-486 groups. Rats in these different groups were treated with agomiR-21 (5  $\mu$ L, 40 nmol/mL), antagomiR-21 (5  $\mu$ L, 40 nmol/mL) or agomiR-NC (5  $\mu$ L, 40 nmol/mL), respectively. In this study, the drugs were administered *via* tail intravenous injection 1 h before modeling.

Briefly, the experimental protocol is as follows [7]. The rats were anesthetized with 1 g/kg urethane (Shanghai Qingxi, Shanghai, China) and ventilated with a respirator (TKR-200C, Jiangxi, China), with a stroke volume of 12 mL/kg and a frequency of 60 times/min. Next, the left chest was cut open by making an incision between the second and fourth ribs. Then, the distal left anterior descending branch was ligated at 1/3 using a 6-0 silk suture with a slipknot, and a small tube was placed between the ligature and the myocardium. The suture was tightened to block the coronary artery, thereby inducing ischemic injury. Rats in sham operation group underwent the same surgical procedures except for ligation of blood vessels. At 24 h after myocardial ischemia, the rats were sacrificed, and the blood samples and heart tissues were collected. Serum were collected from the blood samples after centrifugation. The study was approved by the institutional ethical committee and followed international guidelines for animal studies.

### Assessment of rat cardiac function

The cardiac function was examined *via* electrocardiogram (ECG) throughout ischemia-reperfusion (I/R). A BL-420F hemodynamic

system (Chengdu Taimeng Technology Co., Ltd., Chengdu, China) was used to measure and record left ventricular systolic pressure (LVSP), left ventricular end-diastolic pressure (LVEDP), maximum rate of left ventricular pressure rise ( $+dp/dt_{max}$ ) and maximum rate of left ventricular pressure decrease ( $-dp/dt_{max}$ ).

#### Determination of differentially expressed miRNAs by gene chip assay

Total RNAs were extracted from the bone marrow tissues of rats, and then quantified using a NanoDrop kit (Thermo Fisher Scientific, Waltham, MA, USA). Next, the integrity of RNAs was assessed using a Bioanalyzer 48600 (Agilent, Santa Clara, CA, USA). In this study, 100 ng of total RNAs and an Affymetrix 3' IVT Express kit were used to prepare complimentary RNAs (cRNAs). Thereafter, the cRNAs were hybridized on an Affymetrix Primeview Human microarray at 45°C for 16 h according to the instructions of GeneChip 3' Array (Affymetrix, Santa Clara, CA, USA). In addition, the microarrays were processed on Affymetrix FS-450 fluid station for washing and staining, and scanned using an Affymetrix GeneChip scanner according to the protocol provided by the manufacturer. The raw data of the CEL file were imported into the Partek Genomics Suite 6.6 software, and the probe set was normalized using the Robust Multiarray Average method. The significance of the differentially expressed genes was determined using one-way analysis of variance (ANOVA), and the P was corrected using FDR.

#### Prediction of miRNA target genes

The direct targets of differentially expressed miRNAs were predicted in bulk using the DIANA Tools (<http://diana.imis.athena-innovation.gr/DianaTools/index.php?r=site/index>).

#### Hematoxylin-eosin (H & E) staining

All rats to be tested were sacrificed *via* cervical dislocation, and the hearts were excised, treated with 4 % paraformaldehyde/PBS (pH 7.4) at 4 °C for 48 h, washed with running water, dehydrated with 70, 80, 95 and 100 % ethanol that was removed with xylene, and embedded in paraffin (2 µm). Next, staining was conducted using a H & E staining kit (Beyotime, Shanghai, China) strictly according to the instructions of the kit. The stained sections were observed under the light microscope (BX-42, Olympus, Tokyo, Japan).

#### Determination of apoptosis of myocardial tissues

The prepared paraffin sections were subjected to TUNEL staining in strict accordance with the instructions of the manufacturer's kit to determine the apoptosis level of myocardial tissues in each group of rats. The staining was observed, and the apoptotic cells were brown.

#### Western blotting

An appropriate amount of radio immunoprecipitation assay (RIPA) was taken, added with the protease inhibitor phenylmethylsulfonyl fluoride (PMSF) at a ratio of 100:1 (RIPA: PMSF) and mixed to prepare cell lysis buffer. After trypsinization, the cells were collected and added with lysis buffer, and the resulting product was collected, transferred to an eppendorf (EP) tube, and centrifuged at 4°C and 14,000 rpm for 30 min using a low temperature high-speed centrifuge, followed by collection of the protein supernatant. Thereafter, the proteins were denatured at 95°C for 10 min *via* thermal bath. The prepared protein samples were placed in a refrigerator at -80°C for later use. The proteins were quantified using a bicinchoninic acid (BCA) kit (Pierce, Rockford, IL, USA). After that, the gels for sodium dodecyl sulphate-polyacrylamide gel electrophoresis (SDS-PAGE) were prepared, and the protein samples were loaded into the well of the gels for electrophoresis at constant voltage (80 V) for 2.5 h, followed by semi-dry transfer to a polyvinylidene fluoride (PVDF) membrane (Millipore, Billerica, MA, USA). Afterwards, the membrane was immersed in Tris-buffered saline with Tween®20 (TBST) buffer containing 5 % skim milk powder, and shaken slowly for 1 h for blocking. Then, antibodies were diluted with 5 % skim milk powder, and the membrane was incubated with primary antibodies and rinsed with TBST solution 3 times (10 min/time). Next, the membrane was incubated with a secondary antibody at room temperature for 2 h, and rinsed twice with TBST and once with TBS (10 min/time). Electrochemiluminescence (ECL) reagents were used to detect proteins, with exposure in a dark room. The relative expression levels of proteins [gene of phosphate and tension homology deleted on chromosome ten (PTEN) (ab170941, Abcam, Cambridge, MA, USA), protein kinase B (AKT) (ab18785, Abcam, Cambridge, MA, USA), phosphorylated protein kinase B (p-AKT) (ab38449, Abcam, Cambridge, MA, USA) and glyceraldehyde-3-phosphate dehydrogenase (GAPDH) (ab9484, Abcam, Cambridge, MA, USA)] were analyzed by Image-

Pro Plus v6 (Media Cybernetics, Silver Spring, MD, USA).

### Luciferase reporter assay

In this experiment, wild-type and mutant PTEN in its 3'-UTR were amplified and cloned into psiCHECK-2 luciferase plasmids (Promega, Madison, WI, USA) to generate wild-type PTEN and mutant reporter genes. The HEK293 cells were cultured in a 24-well plate and co-transfected with miR-486 or miR-con and wild-type or mutant plasmids for 48 h. Thereafter, the activity of luciferase was determined using dual-luciferase reporter reagent (Promega, Madison, WI, USA).

**Table 1:** Primer sequences

Primer name	Primer sequence (5'-3')
MiR-93-5p	AGAGTCATCAAGCTTCTGTCTGTGC CACUGAUUUCAAUGGUGCUAUU
MiR-214	TGAAAACGCAGGAGACGACCTC CGAGTGGAATTGCTGTTTCGG
MiR-4503	CTGGTTTCATATGGTGGTTT GAACATGTCTGCGTATCTC
MiR125-5p	GGACTACTTGCACTCCGAGAAG CATAGTGGCACCGTCCTTGATC
PTEN	TGAGTTCCTCAGCCATTGCCT GAGGTTTCTCTGGTCTGGTA
MiR-199a-3p	TGATACGCCTGAGTGGCTGTCT CACAAAGCAGTGAGCGCTGAA
MiR-486	GCTTTGAGGCTGTCTACCAGCT GTGAGGACCTTGACAAGCCACT
MiR-499-5p	GTCCAGATGCTGTACCTTCCTC GCGAGTCTTCTCCTCCAGTAT
MiR-721	CAGTGCAATTAAGGGGAA CTCAACTGGTGTCTGGAGTCG
GAPDH	CATCACTGCCACCCAGAAGACTG ATGCCAGTGAGCTTCCCGTTCAG

### Quantitative reverse transcription-polymerase chain reaction (RT-qPCR)

qRT-PCR was used to determine the expression of differentially expressed miRNAs in bone marrow tissues. Total RNA was extracted using TRIzol® reagent (Invitrogen; Thermo Fisher Scientific, Inc.) according to the manufacturer's protocol. The RT reaction: the samples containing 500 ng of RNAs were divided into three groups, and the total RNAs in each group were diluted 10 times. Total RNAs (3 µL) were taken for PCR amplification. The amplification level of the target genes was verified using 5% agarose gel electrophoresis. The LabWorks 4.0 image acquisition and analysis software was applied for quantitative and data processing. In this study, GAPDH was used as an internal reference. Primers for the miR-126 gene were bought from ABM (Peterborough, Camb, Canada). For each group of samples, three

replicate wells were set to obtain reliable data. In this study, the  $2^{-\Delta\Delta Ct}$  method was used to analyze the changes in relative expression level of the target genes. The primer sequences used in this study are shown in Table 1.

### Statistical analysis

Statistical Package for Social Sciences (SPSS) 19.0 software (IBM, Armonk, NY, USA) was employed for statistical analysis. Data are expressed as mean  $\pm$  standard deviation. Student's *t*-test was used for statistical analysis, and  $p < 0.05$  was considered statistically significant.

## RESULTS

### Screened differentially expressed miRNAs in myocardial tissues of rats in model group

The results of expression profile screening (Figure 1) uncovered the significant difference in miRNA expression profiles in myocardial tissues between model group and sham group. With fold change  $> 0.8$  and  $p < 0.01$  as the screening criteria, 8 miRNAs in myocardial tissues in model group showed significant differences when compared with those in sham operation group, including 5 miRNAs (miR-93-5p, miR-214, miR-4503, miR125-5p and miR-199a-3p) significantly up-regulated and 3 miRNAs (miR-486, miR-499-5p and miR-721) overtly down-regulated.

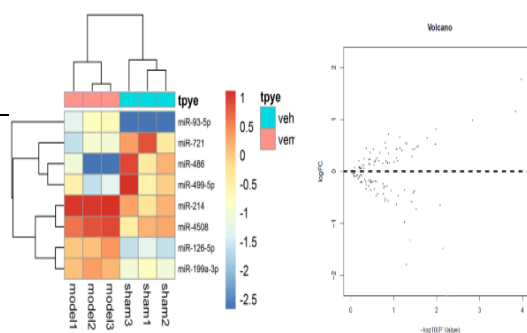


**Figure 1:** Unsupervised cluster analysis heat map (model: myocardial tissues in model group, sham: myocardial tissues in sham operation group, each row for a miRNA, red for a higher expression level and blue for a lower expression level). Significant differences are found in miRNA expression profiles in myocardial tissues between model group and sham operation group

### Differences in the expressions of miRNAs

To further verify the reliability of the high-throughput screening results, the low-throughput RT-qPCR assay was performed in this study to

verify the differentially expressed miRNAs. It was found that the expression levels of the 8 differentially-expressed miRNAs selected in myocardial tissues in model group were significantly different from those in myocardial tissues in sham operation group, and the differences were statistically significant ( $p < 0.01$ ). Among these 8 miRNAs, miR-486 had the largest difference in expression level (Figure 2).

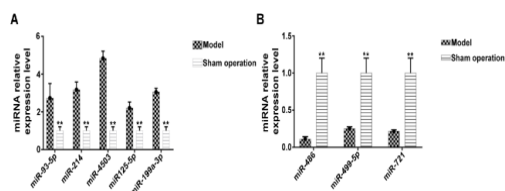


**Figure 2:** Differences in miRNA expressions determined through RT-qPCR ( $**p < 0.01$ , model group vs. sham operation group). Compared with those in myocardial tissues in sham operation group, the expression levels of the 8 differentially expressed miRNAs selected is clearly different in myocardial tissues in model group

### MiR-486 negatively regulated the expression of PTEN by directly binding to the 3'-UTR of PTEN mRNA

Based on biological information predictions, PTEN may be a potential target of miR-486 (Figure 3 A). To further confirm the interaction between miR-486 and PTEN, luciferase reporter assay was employed in this study to determine the response of wild-type PTEN and mutant PTEN to miR-486 and miR-con in HEK293 cells (Figure 3 B). The results showed that the fluorescence response intensity of HEK293 cells with wild-type PTEN transfected with miR-486 was remarkably weakened, while that of HEK293 cells with mutant PTEN had no evident changes. To obtain further evidence, RT-qPCR and Western blotting were performed in this study, and it was found that transfection with miR-486 significantly lowered the protein and mRNA levels of PTEN; and on the contrary, knocking down miR-486 increased the PTEN gene expression (Figures 3 C - E). These above results suggest that miR-486 negatively regulated the PTEN expression by binding to the 3'UTR of PTEN mRNA.

### Effect of miR-486 expression level on the content of myocardial enzymes in rat serum

The expression level of miR-486 in rat myocardial tissues was overtly lower in model group than that in sham group, and it declined markedly in antagomiR-486 group ( $p < 0.01$ ). The serum content of lactate dehydrogenase

(LDH), creatinine kinase (CK) and Troponin T (TnT) in rats were increased significantly in model group when compared with that in sham operation group ( $p < 0.01$ ), suggesting that myocardial tissue damage in rats is aggravated in model group. Compared with that in the model group, it was significantly reduced in agomiR-486 group ( $p < 0.01$ ) and significantly increased in antagomiR -486 group. These results imply that miR-486 alleviates myocardial injury in rats in a dose-dependent manner (Figure 4).

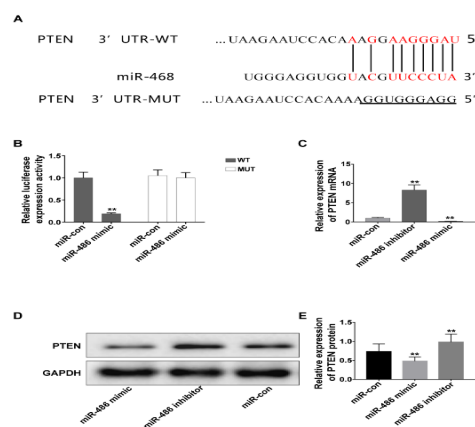


**Figure 3:** MiR-486 negatively regulates the expression of PTEN by directly binding to the 3'-UTR of PTEN mRNA. (A) Direct binding sites of miR-486 to the 3'-UTR of PTEN mRNA predicted using bioinformatics software; (B) Response of wild-type and mutant PTEN to miR-486 mimic and miR-con in HEK293, determined using luciferase reporter assay; (C, D, E) Effects of transfection with miR-con, miR-486 mimic and miR-486 inhibitor on the mRNA and protein levels of PTEN, determined through Western blotting and RT-qPCR;  $**p < 0.01$ , miR-486 mimic group vs. miR-con group;  $&&p < 0.01$  miR-486 inhibitor group vs. miR-con group

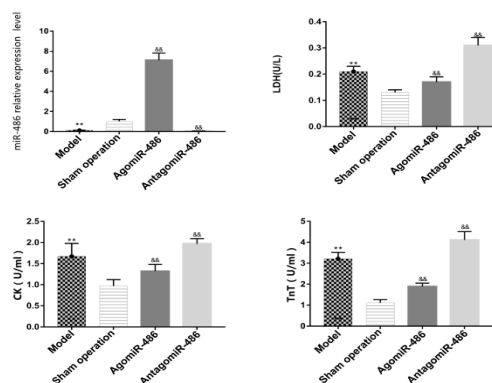


**Figure 4:** Effect of miR-486 expression level on myocardial enzyme content in rat serum.  $**p < 0.01$ , model group vs. sham operation group,  $&&p < 0.01$ , agomiR-486 and antagomiR-486 group vs. model group. MiR-486 reduce the level of myocardial injury in a dose-dependent manner

### Effect of miR-486 expression level on the cardiac function of rats

The effect of miR-486 expression level on cardiac function in rats after I/R injury shown in Table 2 revealed that the LVSP,  $+dp/dt_{max}$  and  $-dp/dt_{max}$  of rats were lower in model group than those in sham operation group, while the LVEDP was significantly higher in model group than in the sham operation group, ( $p < 0.01$ ). Compared with the model group, agomiR-486 group had significantly raised LVSP,  $+dp/dt_{max}$  and  $-dp/dt_{max}$  and evidently decreased LVEDP, ( $p < 0.01$ ), and antagomiR-486 group displayed markedly declined LVSP,  $+dp/dt_{max}$  and  $-dp/dt_{max}$  and elevated LVEDP ( $p < 0.01$ ), implying that agomiR-486 can overtly improve the weakened heart function caused by AMI.

### Effect of miR-486 expression level on myocardial morphology of rats

According to H & E staining results, sham operation group had regularly arranged myocardial cells with normal size and morphology, without infarct lesions. In model group, myocardial cells were disorderly arranged, different in size, with some myofibrosis and muscle fiber swelling and infiltration of many inflammatory cells. In agomiR-486 group, there was a better protection on myocardium, and it was observed that there were neatly arranged myocardial cells with uniform staining and clear boundaries between cells, without interstitial edema, and inflammatory cell infiltration was mitigated when compared with that in model group. AntagomiR-486 group displayed significantly deteriorated morphology in myocardial tissues of rats (Figure 5).

### Effect of miR-486 expression level on myocardial apoptosis level

The results of Western blotting (Figure 6 A) revealed that compared with those in model group, the expression levels of apoptosis-related proteins (active-caspase 3 and active-caspase 9) in myocardial tissues overtly declined in agomiR-

486 group ( $p < 0.01$ ) and significantly rose in antagomiR-486 group ( $p < 0.01$ ). TUNEL assay results showed that the level of myocardial apoptosis was obviously higher in model group than that in sham operation group. Compared with that in model group, the TUNEL-positive rate in rat myocardial tissues was evidently reduced in agomiR-486 group, while it was clearly raised in antagomiR-486 group (Figure 6 B). These results suggest that miR-486 reduce the myocardial apoptosis level in rats in a dose-dependent manner.

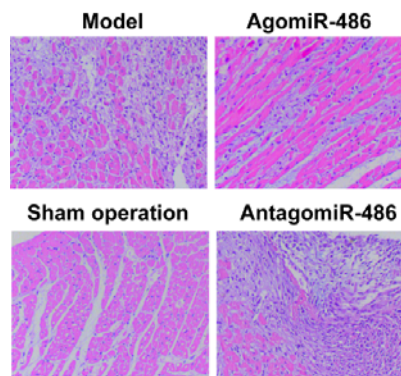


**Figure 5:** Effect of miR-486 expression level on the morphology of heart tissues of rats with I/R injury, detected via staining assay ( $\times 400$ ) In agomiR-486 group, the myocardium were protected better, and inflammatory cell infiltration were relieved when compared with that in model group

### Effect of miR-486 expression level on the PTEN/AKT signaling pathway

To further explore the molecular mechanism of miR-486 in affecting the myocardial apoptosis, Western blotting was adopted in this study to investigate the effect of agomiR-486 on the PI3K/AKT signaling pathway. The experimental results revealed that the protein expression levels of PTEN and p-AKT/AKT in rat myocardial tissues were remarkably lower in model group than those in sham operation group, showing statistically significant differences ( $p < 0.01$ ).

**Table 2:** Effect of miR-486 expression level on cardiac function of rats

Group	LVSP (mm Hg/s)	LVEDP (mm Hg/s)	$+dp/dt_{max}$ (mm Hg/s)	$-dp/dt_{max}$ (mm Hg/s)
Sham	95 $\pm$ 11	4.3 $\pm$ 0.8	6732 $\pm$ 397	5931 $\pm$ 623
Model	49 $\pm$ 8**	9.3 $\pm$ 2.3###	5640 $\pm$ 513###	4731 $\pm$ 503###
AgomiR-486	80 $\pm$ 7.3&&	5.6 $\pm$ 1.6&&	6510 $\pm$ 670&&	5269 $\pm$ 454&&
AntagomiR-486	37 $\pm$ 5.1&&	11.2 $\pm$ 2.1&&	5431 $\pm$ 5486&	4127 $\pm$ 379&&

### $P < 0.01$  model group vs. sham group; \*\* $p < 0.01$  model group vs. sham operation group; && $p < 0.01$  agomiR-486 and antagomiR-486 group vs. model group. MiR-486 improve cardiac function indices of rats in a dose-dependent manner

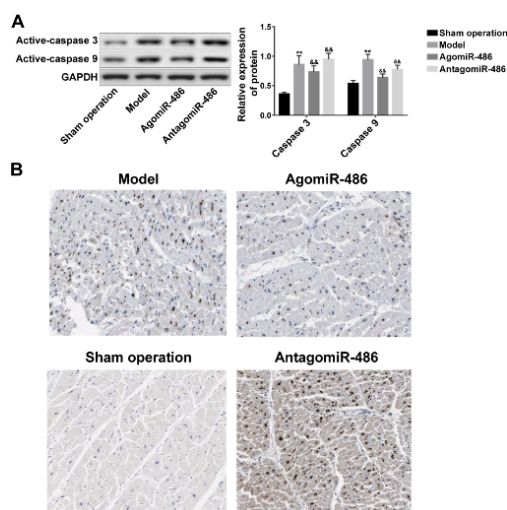


**Figure 6:** (A) Effect of miR-486 expression level on myocardial apoptosis level ( $\times 400$ )  $^{**}p < 0.01$  model group vs. sham operation group,  $\&\&p < 0.01$  agomiR-486 and antagomiR-486 group vs. model group. (B) MiR-486 ameliorates the myocardial apoptosis level in rats in a dose-dependent manner

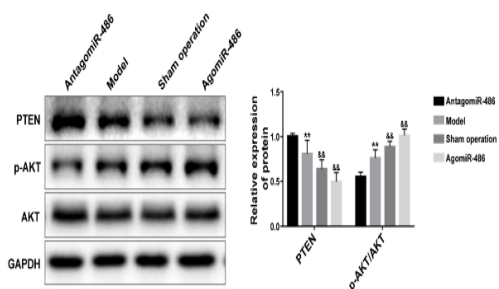


**Figure 7:** Effects of miR-486 expression level on the expression levels of the PI3K/AKT signaling pathway and its downstream proteins. Compared with model group, agomiR-486 group have a clearly elevated protein expression level of p-AKT/AKT and a significantly reduced protein expression level of PTEN.  $\&\&p < 0.01$ , model group vs. agomiR-486 and antagomiR-486 group;  $^{**}p < 0.01$ , model group vs. sham operation group

Compared with the model group, agomiR-486 group exhibited a clearly elevated protein expression level of p-AKT/AKT, and a significantly reduced protein expression level of PTEN, and the differences were of statistical significance ( $p < 0.01$ ), while antagomiR-486 group had a markedly decreased protein expression level of p-AKT/AKT and a distinctly raised protein expression level of PTEN, and the differences were statistically significant ( $p < 0.01$ ). The above results point out that miR-486 down-regulates the protein expression level of PTEN to activate the AKT signaling pathway, thus protecting against myocardial infarction in rats (Figure 7).

## DISCUSSION

Coronary heart disease is one of the diseases with the highest mortality rates in the world. Thrombolytic therapy or PCI intervention is the most effective strategy to improve clinical outcomes. However, in the case of AMI, the mortality rate is close to 10 %, and the incidence rate of heart failure is almost 25 %, despite all the protective measures adopted on the myocardium [7-9]. Apoptosis is an important program modulating programmed cell death. Decreasing the myocardial apoptosis rate in the infarction area is beneficial for the improvement of the mortality rate and adverse reactions of patients with AMI.

In this study, 8 differentially-expressed genes in rat myocardial tissues in model group were screened out *via* gene-chip and RT-qPCR assays. These comprised 5 significantly up-regulated miRNAs (miR-93-5p, miR-214, miR-4503, miR125-5p and miR-199a-3p) and 3 overtly down-regulated miRNAs (miR-486, miR-499-5p and miR-721). Many of these genes have been proven to play vital roles in the pathophysiological process of AMI. For example, Liu *et al* [7] pointed out that miR-93-5p can target ATG7 and TLR4 to evidently repress hypoxia-induced autophagy and inflammatory cytokine expression, thus relieving myocardial damage induced by AMI. Research conducted by Yin *et al* [10] discovered that the expression level of miR-214 rose remarkably in the serum of elderly AMI patients, and miR-214 inhibited the apoptosis of myocardial cells by suppressing the expression of its target genes. A study by Xue *et al* [11] uncovered that miR-199a is markedly elevated in patients with AMI, which is of high diagnostic efficiency in the prediction of AMI. Moreover, research by Yan *et al* [12] revealed that miR-199a-5p targets JunB to induce the apoptosis of H9C2 myocardial cells.

Among the 3 down-regulated differentially expressed miRNAs, miR-486 has the largest difference in expression level. Currently, the studies on miR-486 in AMI are rare. Some of these studies have demonstrated that the difference in the expression level of miR-486 in AMI patients can be used to predict the development of AMI [13-15]. Furthermore, a study by Zhang *et al* [15] suggested that miR-486 target NDRG2 to inactivate the JNK/c-jun and NF- $\kappa$ B signaling pathways, thereby ameliorating hypoxia-induced apoptosis of H9C2 cells [16]. It was discovered in this study that miR-486 improved the cardiac function of rats and the morphology of myocardial tissues, and reduced AMI-induced apoptosis of myocardial cells and

the expression of myocardial enzymes (markers of myocardial injury) in a dose-dependent manner. The results of the luciferase reporter gene assay showed that PTEN was a direct target of miR-486. The results of Western blotting analysis pointed out that raised expression of miR-486 in rat models of AMI remarkably suppressed the protein expression level of PTEN and up-regulated that of p-AKT/AKT.

The AKT signaling pathway is a downstream signaling pathway of the RAS-Raf signaling pathway. The binding of PI3K to Ras protein is able to phosphorylate PIP2 into PIP3 that then binds to the PH domain of AKT protein to phosphorylate AKT protein. The phosphorylated AKT protein is capable of phosphorylating a series of substrates. Besides, the phosphorylated AKT protein has a series of important biological functions that include inhibiting apoptosis, stimulating cell proliferation and growth, and affecting cell migration and angiogenesis [17]. The expression level of messenger molecule PIP3 in resting cells is very low, and is regulated by PTEN protein. PTEN converts active molecule PIP3 to PIP2, thereby inhibiting the phosphorylation of AKT protein. In addition, PTEN regulates myocardial apoptosis during AMI, and improves cardiac function, and thus plays a crucial role in the process of AMI [18,19].

## CONCLUSION

MiR-486 targets PTEN and activates the AKT signaling pathway to exert a protective role in AMI rats. The results of the current study may provide a new insight into the development of suitable therapies for AMI.

## DECLARATIONS

### Conflict of interest

No conflict of interest is associated with this work.

### Contribution of authors

We declare that this work was done by the authors named in this article and all liabilities pertaining to claims relating to the content of this article will be borne by the authors.

### Open Access

This is an Open Access article that uses a funding model which does not charge readers or their institutions for access and distributed under the terms of the Creative Commons Attribution

License (<http://creativecommons.org/licenses/by/4.0>) and the Budapest Open Access Initiative (<http://www.budapestopenaccessinitiative.org/read>), which permit unrestricted use, distribution, and reproduction in any medium, provided the original work is properly credited.

## REFERENCES

1. Reed GW, Rossi JE, Cannon CP. Acute myocardial infarction. *Lancet* 2017; 389(10065): 197-210.
2. Zang X, Qi X. Association Between PM2.5 Exposure and the Prognosis of Patients with Acute Myocardial Infarction. *Arch Med Res* 2017; 48(3): 292-296.
3. Sun HY, Wang XL, Ma LC, Yang M, Yang HJ, Huang HW, Zhao GA. Influence of MiR-154 on myocardial apoptosis in rats with acute myocardial infarction through Wnt/beta-catenin signaling pathway. *Eur Rev Med Pharmacol Sci* 2019; 23(2): 818-825.
4. Wang C, Jing Q. Non-coding RNAs as biomarkers for acute myocardial infarction. *Acta Pharmacol Sin* 2018; 39 (7): 1110-1119.
5. Yu BT, Yu N, Wang Y, Zhang H, Wan K, Sun X, Zhang CS. Role of miR-133a in regulating TGF-beta1 signaling pathway in myocardial fibrosis after acute myocardial infarction in rats. *Eur Rev Med Pharmacol Sci* 2019; 23(19): 8588-8597.
6. Jin Y, Ni S. miR-496 remedies hypoxia reoxygenation-induced H9c2 cardiomyocyte apoptosis via Hook3-targeted PI3k/Akt/mTOR signaling pathway activation. *J Cell Biochem* 2020; 121(1): 698-712.
7. Liu J, Jiang M, Deng S, Lu J, Huang H, Zhang Y, Gong P, Shen X, Ruan H, Jin M, Wang H. miR-93-5p-Containing Exosomes Treatment Attenuates Acute Myocardial Infarction-Induced Myocardial Damage. *Mol Ther Nucleic Acids* 2018; 11: 103-115.
8. Raj P, McCallum JL, Kirby C, Grewal G, Yu L, Wigle JT, Netticadan T. Effects of cyanidin 3-O-glucoside on cardiac structure and function in an animal model of myocardial infarction. *Food Funct* 2017; 8(11): 4089-4099.
9. Tektonidis TG, Akesson A, Gigante B, Wolk A, Larsson SC. A Mediterranean diet and risk of myocardial infarction, heart failure and stroke: A population-based cohort study. *Atherosclerosis* 2015; 243(1): 93-98.
10. Yin Y, Lv L, Wang W. Expression of miRNA-214 in the sera of elderly patients with acute myocardial infarction and its effect on cardiomyocyte apoptosis. *Exp Ther Med* 2019; 17(6): 4657-4662.
11. Xue S, Zhu W, Liu D, Su Z, Zhang L, Chang Q, Li P. Circulating miR-26a-1, miR-146a and miR-199a-1 are potential candidate biomarkers for acute myocardial infarction. *Mol Med* 2019; 25(1): 18.
12. Yan M, Yang S, Meng F, Zhao Z, Tian Z, Yang P. MicroRNA 199a-5p induces apoptosis by targeting JunB. *Sci Rep* 2018; 8(1): 6699.
13. Zhang X, Zhang C, Wang N, Li Y, Zhang D, Li Q. MicroRNA-486 Alleviates Hypoxia-Induced Damage in *Trop J Pharm Res*, September 2021; 20(9): 1852



- H9c2 Cells by Targeting NDRG2 to Inactivate JNK/C-Jun and NF-kappaB Signaling Pathways. *Cell Physiol Biochem* 2018; 48(6): 2483-2492.
14. Hsu A, Chen SJ, Chang YS, Chen HC, Chu PH. Systemic approach to identify serum microRNAs as potential biomarkers for acute myocardial infarction. *Biomed Res Int* 2014; 2014: 418628.
  15. Zhang R, Lan C, Pei H, Duan G, Huang L, Li L. Expression of circulating miR-486 and miR-150 in patients with acute myocardial infarction. *BMC Cardiovasc Disord* 2015; 15: 51.
  16. Wei T, Folkersen L, Ehrenborg E, Gabrielsen A. MicroRNA 486-3P as a stability marker in acute coronary syndrome. *Biosci Rep* 2016; 36(3): e00351.
  17. Hennessy BT, Smith DL, Ram PT, Lu Y, Mills GB. Exploiting the PI3K/AKT pathway for cancer drug discovery. *Nat Rev Drug Discov* 2005; 4(12): 988-1004.
  18. Wu L, Chen Y, Chen Y, Yang W, Han Y, Lu L, Yang K, Cao J. Effect of HIF-1alpha/miR-10b-5p/PTEN on Hypoxia-Induced Cardiomyocyte Apoptosis. *J Am Heart Assoc* 2019; 8(18): e11948.
  19. Yin Y, Lv L, Wang W. Expression of miRNA-214 in the sera of elderly patients with acute myocardial infarction and its effect on cardiomyocyte apoptosis. *Exp Ther Med* 2019; 17(6): 4657-4662.